ELSEVIER

Polymer 44 (2003) 289–293

polymer

www.elsevier.com/locate/polymer

Intercalated polypyrrole/Na^+-montmorillonite nanocomposite via an inverted emulsion pathway method

J.W. Kim[a], F. Liu[a], H.J. Choi[a,*], S.H. Hong[b], J. Joo[b]

[a]*Department of Polymer Science and Engineering, Inha University, Incheon 402-751, South Korea*
[b]*Department of Physics, Korea University, Seoul 136-701, South Korea*

Received 20 May 2002; received in revised form 29 August 2002; accepted 13 September 2002

Abstract

An inverted emulsion pathway polymerization method was introduced to synthesize conducting polypyrrole (PPy) into the layer of inorganic clay within a nanolevel, using dodecylbenzenesulfonic acid (DBSA) as both an emulsifier and a dopant. The synthesized PPy/Na^+-montmorillonite (MMT) nanocomposite was confirmed to have a layered structure with a folded or penetrated PPy from X-ray diffraction, and it was further characterized via FT-IR spectroscopy. Four probes method was adopted to examine electrical DC conductivity. Electrorheological (ER) behavior of the nanocomposite dispersed in silicone oil was also investigated using a rotational rheometer equipped with a high voltage generator.

Keywords: Conducting polymer; Polypyrrole; Nanocomposite

1. Introduction

Polypyrrole (PPy) is a promising conducting polymeric material for various electronic applications such as light emitting diode [1], organic FET [2], EMI shielding [3], and the secondary battery [4], because of its environmental stability to oxygen and water, high conductivity and ease of synthesis [5]. Furthermore, suspension of the PPy in an electrically insulating silicone oil was introduced as an electrorheological (ER) fluid [6]. As one of the most spectacular smart and intelligent materials, ER fluids, which commonly are suspensions of micron-sized particles possessing a higher dielectric constant and/or conductivity than that of suspending fluids in a nonconducting fluid, exhibit reversible changes in their rheological properties as a function of electric field strength [7]. In the presence of a strong electric field, the suspended particles attract each other to form a solid-like network of fibers aligned in the field direction. Various polarizable semiconducting polymers including polyaniline (PANI) [8,9], copolyaniline [10,11], polypyrrole [12], poly(acene quinine) radicals [13] and phosphate cellulose [14] are developed as dry-base ER materials.

The PPy and its derivatives have been synthesized either by an electrochemical or by a chemical oxidative polymerization. Generally, PPys are brittle, insoluble and infusible, and hence inprocessible. Thereby, in order to develop Ppy-based conductive materials, several approaches including oxidant-impregnated polymerization using pyrrole vapor [15], electrochemical polymerization of pyrrole in the presence of latex particles with anionic surface [16], and graft copolymerization containing pyrrole as grafted groups [17], have been applied. Furthermore, Ruckenstein and Hong [18] introduced two emulsion pathways to synthesize Ppy-based conductive composites.

Meanwhile, nanostructured hybrid polymer/clay nanocomposites have attracted considerable attention for various engineering applications such as enhanced mechanical property and thermal stability, reduced gas permeability, and self-extinguishing flame retardant characteristics [19–24]. In the case of conducting polymer/inorganic clay nanocomposites, they provide the new synergistic properties, which cannot attain from individual materials, such that the conductivity (σ) is more easily controlled, and the mechanical or thermal stability is improved through the synthesis of the nanocomposites. On the other hand, as one of the preparation methods to fabricate polymer nanocomposite, emulsion polymerization has been used to produce various nanocomposites consisting of PANI [25,26],

* Corresponding author. Tel.: +82-32-860-7486; fax: +82-32-865-5178.
E-mail address: hjchoi@inha.ac.kr (H.J. Choi).

0032-3861/03/$ - see front matter © 2002 Published by Elsevier Science Ltd.
PII: S0032-3861(02)00749-8

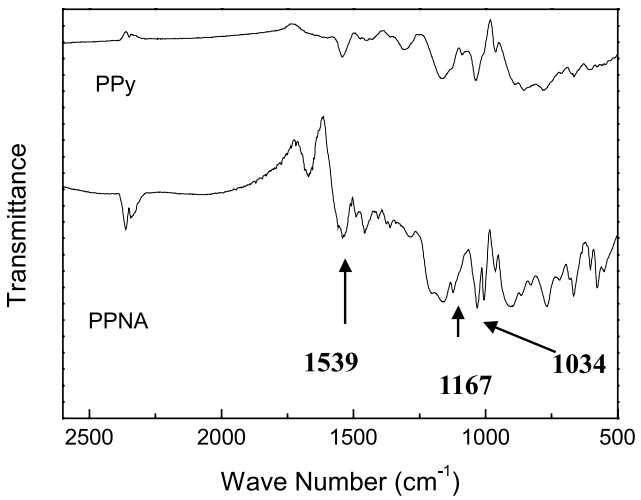

Fig. 1. FT-IR diagrams of PPy and PPNA samples.

polystyrene [27] or styrene/acrylonitrile copolymer [28] and Na^+-montmorillonite (MMT). Since the interlayers of Na^+-MMT are filled with sodium cations, the hydrophilic properties are enhanced and lead to a high degree of swelling in water. These phenomena hence provide an effective method for the preparation of intercalated nanocomposites if aqueous systems are used during the intercalation procedure. Nanocomposites with PANI and styrene/acrylonitrile copolymer have also been used as suspending particles for ER fluids [25,28,29]. Furthermore, PANI/clay nanocomposites are adopted in the areas of corrosion protection [30] and enhanced electrical conductivity [31].

In this study, we synthesize the PPy/clay nanocomposite (PPNA) particles via an inverted emulsion pathway polymerization which has been introduced by previous investigators [17,32], and characterize their physical and chemical properties. We also prepare an electrorheological (ER) fluid using synthesized nanocomposite and measure its rheological properties under high electric field applied.

2. Experimental part

2.1. Synthesis of nanocomposite

In this inverted emulsion polymerization of PPNA nanocomposite, DBSA was used as both a dopant and an emulsifier. Initially, DBSA (6.0 mol) was dissolved in isooctane (900 g), and it was mixed with ammonium peroxysulfate (0.03 mol) solution in distilled water (24 ml) for 1 h. Once the inverse emulsion formed, it was mixed with Na^+-MMT (Southern Clay Products, USA) dispersed in 24 ml distilled water for 12 h at 0 °C [33]. The weight ratio of Na^+-MMT was fixed to be 15% in the final product of the PPNA nanocomposite. This is referred to be inverted emulsion, which is opposed to the conventional oil-in-water emulsion. Pyrrole monomer (4 g) solution in toluene was then dropped into the reactor for 30 min. Reaction temperature was kept at 0 °C for 24 h. Excess acetone was then introduced into the reaction mixture to terminate the reaction. Prior to use as an ER fluid, pH of the product was adjusted to be 10 by adding either NaOH or HCl solution for dedoping. Finally, we obtained the particles for the ER application by washing, filtering, drying, milling, and sieving, sequentially.

2.2. Characterization

After synthesis, the insertion of PPy into the layers was examined using X'pert-MPD (Phillips, model pw 3020, $\lambda = 1.542$ Å) diffractometer, operated at 40 kV and 30 mA, in which powder form of the PPNA nanocomposite was placed on the glass for the XRD experiments. Chemical structure of the materials was characterized by FT-IR spectrometer (Bio-Rad, FTS-60, USA). Shape and size of the particles were determined by scanning electron microscope (Hitach S-4300, Japan). Average particle size of the PPNA particle was about 10–20 μm with irregular shape. A four-probe method and a Janis closed-cycle refrigerator system were also used for measuring temperature dependence of electrical conductivity, $\sigma_{dc}(T)$, from 300 to 10 K. For the $\sigma_{dc}(T)$ measurement, the samples were prepared with pellet form under the pressure of 2.1×10^7 Pa using a hydro-press.

To characterize its ER characteristics, the ER fluids were prepared by dispersing the synthesized PPNA particles in silicone oil (kinematic viscosity: 30 cS) using a mechanical stirrer (1500 rpm). The concentration of particle was 10 wt%. Rheological properties such as shear stress, shear viscosity and yield stress were measured by a rotational rheometer (Physica, MC-120, Germany) with a Couette type cylinder (Z3-DIN) and a high voltage generator (Meyport 230, USA), which can supply DC electric fields (0–10 kV/mm) to the insulated bob. In order to obtain reproducible data, each ER fluid was redispersed at least two or three times prior to measurement. The shear rate was varied from 10^{-2} to 10^3 s, and yield stresses for the prepared ER fluids were mainly obtained under flow in a controlled shear rate (CSR) experiment. The stress of the transition point at which shear viscosity abruptly decreased was interpreted as the yield stress. Flow curves for each ER fluid were determined in the CSR mode, and static yield stresses were obtained in controlled shear stress mode. To obtain an equilibrium internal structure of the particles, an electric field was applied to the ER fluids for 3 min before the rheological measurements were recorded. All measurements were taken at 25 °C unless specified.

3. Results and discussion

Fig. 1 shows the FT-IR spectrum of both PPy and PPNA sample. The peaks at 1539 cm^{-1} (C=C stretching), and

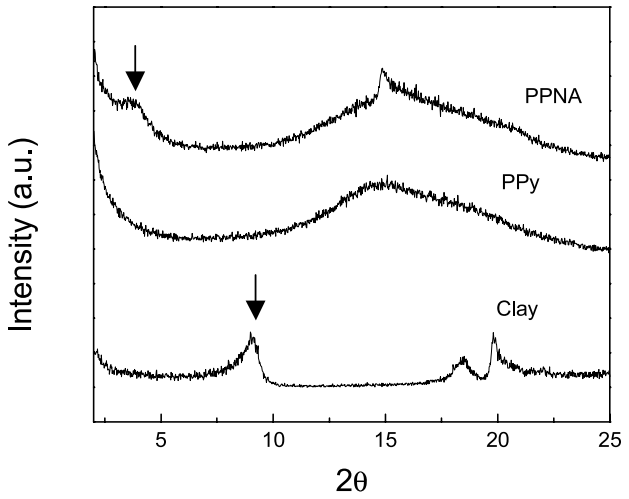

Fig. 2. X-ray diffraction patterns of clay(Na^+-MMT), PPy and PPNA samples.

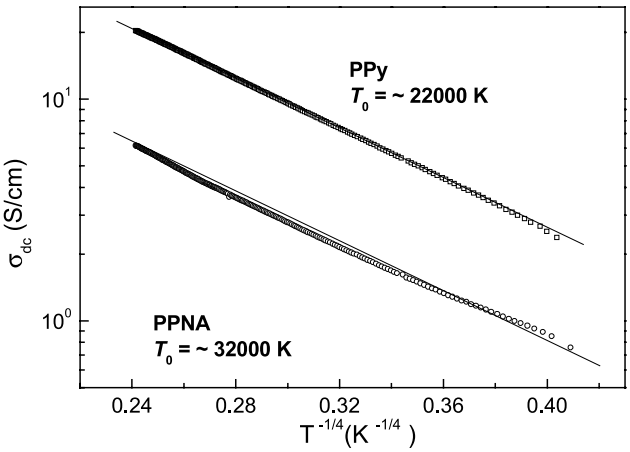

Fig. 3. Temperature dependence of DC conductivity [$\sigma_{dc}(T)$] for PPy and PPNA samples.

1034 cm^{-1} (C–H vibration), shown in PPNA system are the characteristic absorption peaks of PPy sample. The peak at 1167 cm^{-1} is from S=O stretching vibration of sulfonic acid. Thereby, the characteristic peaks of PPy observed in PPNA system shows the intercalation of PPy in the PPNA system.

Insertion of the PPy into the layer of clay was also examined by an XRD, which confirmed that the PPy chain was aligned with the layers of clay. Fig. 2 represents XRD patterns of the clay, PPy and PPNA samples, respectively. The crystalline peak at 8° corresponds to the periodicity in the direction of (001) of the Na^+-MMT samples. The (001) peak was shifted toward a lower angle due to the intercalation of PPy material between the clay layers during nanocomposite synthesis. The variation of d-spacing in the direction of (001) was estimated by using Bragg formula $n\lambda = 2d \sin\theta$. The d-spacing in the direction of (001) of the pristine clay samples is 11.05 Å, and that of PPNA is about to be 16.0 Å, without crystalline peak at 8°. These results demonstrate the intercalation of conducting PPy materials between the clay layers [34].

Fig. 3 represents temperature dependence of DC conductivity [$\sigma_{dc}(T)$] of both PPy and PPNA samples. The σ_{dc} of the PPNA samples was measured to be ~6 S/cm, while that of PPy samples was ~20 S/cm at room temperature by a four probe method. Temperature dependence of σ_{dc} of the PPNA systems follows three-dimensional (3D) variable range hopping (VRH) model, which is described as [35]

$$\sigma_{dc}(T) = \sigma_0 \exp[-(T_0/T)^{1/4}]. \quad (1)$$

Here σ_0 is the proportionality constant of conductivity and $T_0 = 16/[L^3 N(E_F) k_B]$, where L is the localization length, $N(E_F)$ is the density of states at the Fermi level, and k_B is the Boltzmann constant. From the slope of $\sigma_{dc}(T)$, the calculated values of T_0 for the PPy and PPNA samples are ~22 000 and ~32 000 K, respectively. This indicates that the PPy sample has a higher conducting state than the PPNA sample [35]. Based on this result we consider that the molecular structure of PPy is a network structure with side chains and interchain links formed from the main chain, resulting in the 3D VRH model [5,36]. The results are different from the $\sigma_{dc}(T)$ of PANI/clay nanocomposites, in which $\sigma_{dc}(T)$ follows the quasi-1D VRH model [31]. Furthermore, the clay layers are regarded to interrupt the effective doping and weaken the interchain interaction of polymer main chains resulting in low σ_{dc} of the nanocomposite systems.

Fig. 4(a) and (b) shows that the flow curve of shear stress vs. shear rate curve for the PPNA-based ER fluid and shear viscosity vs. shear rate for Ppy-based ER fluids on the electric field, respectively. For an ER measurement, we dedoped the PPNA particle, and then adjusted its conductivity to be 1.2×10^{-8} S/cm. As the shear rate increases, the behavior of shear stress decreased initially and then increased above a critical shear rate as shown in Fig. 4(a) [34]. Extraordinary flow curves with the appearance of a minimum may be the result of structural change of the ER fluid due to shear flow. The particle chains, which are formed by the electric field, are disrupted by the shear flow. When the shear rate becomes high enough, the particle chains may be broken by the shear and the particles may not have enough time to realign themselves along the electric field. Furthermore, the decrease in shear stress with increasing shear rate was reported to occur only under direct current electric fields [37].

On the other hand, the shear stress enhancement is due to the fibril structure of particle formed by an applied electric field. When the shear deformation is applied, the fibrils begin to break apart and reform repeatedly, depending on the magnitude of the applied shear and the particle–particle interaction in the fibrils. It indicates that the PPNA-based ER fluid loses its ER property and follows the Newtonian behavior as the chain structure breaks with a high

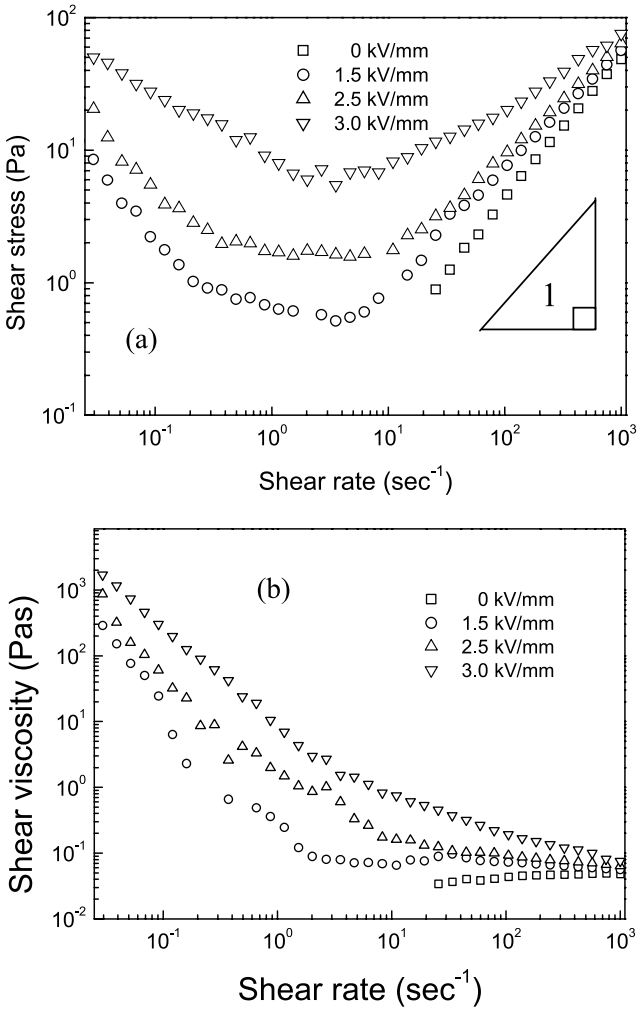

Fig. 4. (a) Shear stress vs. shear rate curves and (b) shear viscosity vs. shear rate curves for PPNA-based ER fluid at various electric fields.

deformation rate. Nonetheless, the PPNA-based ER fluid follows general ER tendency such that shear stress increases with an electric field. Fig. 4(b) shows the shear viscosity of PPNA-based ER suspension with various electric fields. The shear viscosity decreases with the shear rate, similar to shear thinning behavior found in polymer melts or solutions [38].

Furthermore, Fig. 5 indicates that the τ_y is proportional to E^2 for low E, and then τ_y follows abruptly to $E^{3/2}$ for high E, in which the E is an applied electric field. It is well known that τ_y approximately obeys the power behavior, $\tau_y \propto E^{\beta}$ in which the exponent depends on the E range; it is 2 until the E reaches the critical electric field strength E_c, and then generally becomes smaller than 2 as $E > E_c$ as shown in Fig. 5. The E_c of the PPNA-based ER fluid in this study is estimated to be 1.5 kV/mm. The nonlinear conductivity effect with the bulk conducting particle model has been considered and a yield stress model was obtained, showing that the power law index approaches 3/2 at high E [39].

To represent the yield stress data for a broad electric field strength range, Choi et al. [39] conjectured the simple

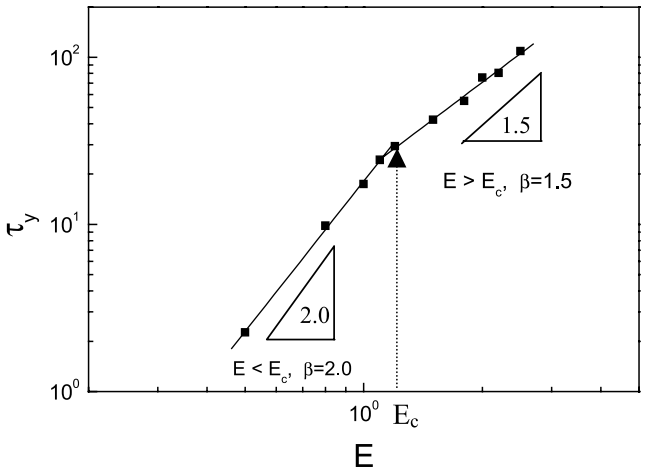

Fig. 5. Yield stress as a function of applied electric fields for PPNA-based ER fluids.

hybrid yield stress equation between τ_y and E

$$\tau_y(E) = \alpha E^2 \left(\frac{\tanh\sqrt{E/E_c}}{\sqrt{E/E_c}} \right), \tag{2}$$

where α depends on the dielectric constant of the fluid and particle volume fraction, and E_c is proportional to the particle conductivity. τ_y in Eq. (2) has two limiting behaviors: E^2 for $E \ll E_c$ and $E^{1.5}$ for $E \gg E_c$, thus showing that the yield stress of the PPNA-based ER fluid follows the simple hybrid yield stress Eq. (2). The behavior of nonlinearity for yield stress has been examined for different ER materials such as poly(*p*-phenylene) and polyaniline [40,41].

In conclusion, we synthesized PPNA particles via an inverted emulsion polymerization for the first time and examined its various characteristics including ER property. Intercalation of PPy was observed from the XRD and FT-IR analysis, in which the characteristic peaks of PPy in the PPNA were observed. Since the existence of clay effects as an insulating material, the conductivity of PPNA was lower than that of pure PPy in a broad range of temperature. Furthermore, the PPNA particle shows not only a typical ER behavior with electric fields but also the existence of a critical electrical field when the yield stress of PPNA-based ER fluids was plotted as a function of an electric field.

Acknowledgements

This work was supported by grant from the KOSEF through Applied Rheology Center at Korea University, Korea.

References

[1] Kilmartin PA, Wright GA. Electrochim Acta 2001;46:2787–94.

[2] Hatfield JV, Covington JA, Gardner JW. Sens Actuators B: Chem 2000;65:253–6.
[3] Lee CY, Lee DE, Joo J, Kim MS, Lee JY, Jeong SH, Byun SW. Synth Met 2001;119:429–30.
[4] Otero TF, Cantero I, Grande H. Electrochim Acta 1999;44:2053–9.
[5] Calvo PA, Rodríguez J, Grande H, Mecerreyes D, Pomposo JA. Synth Met 2002;126:111–6.
[6] Wu S, Zang F, Shen J. Polym J 1998;30:451–4.
[7] Kim JW, Choi HJ, Lee HG, Choi SB. J Ind Engng Chem 2001;7: 218–22.
[8] Choi HJ, Kim TW, Cho MS, Kim SG, Jhon MS. Eur Polym J 1997;33: 699–703.
[9] Hao T. Adv Mater 2001;13:1847–57.
[10] Cho MS, Choi HJ, To K. Macromol Rapid Commun 1998;19:271–3.
[11] Choi HJ, Kim JW, To K. Polymer 1999;40:2163–6.
[12] Kim YD, Park DH. Colloid Polym Sci 2002;280:828–34.
[13] Sohn JI, Cho MS, Choi HJ, Jhon MS. Macromol Chem Phys 2002; 203:1135–41.
[14] Kim SG, Choi HJ, Jhon MS. Macromol Chem Phys 2001;202:521–6.
[15] Makhlouki M, Berne'de JC, Morsli M, Bonnet A, Conan A, Lefrant S. Synth Met 1994;62:101–6.
[16] François G, Siyu Y, Guylaine L, Daniel B. J Electroanal Chem 1992; 334:35–55.
[17] Nazzal AI, Street GB. J Chem Soc, Chem Commun 1985;375–6.
[18] Ruckenstein E, Hong L. Synth Met 1994;66:249–56.
[19] Alexandre M, Beyer G, Henrist C, Cloots R, Rulmant A, Jerome R, Dubois P. Macromol Rapid Commun 2001;22:643–6.
[20] Rong J, Jing Z, Li H, Sheng M. Macromol Rapid Commun 2001;22: 329–34.
[21] Lim ST, Hyun YH, Choi HJ, Jhon MS. Chem Mater 2002;14: 1839–44.
[22] Reichert P, Hoffmann B, Bock T, Thomann R, Mülhaupt R, Friedrich C. Macromol Rapid Commun 2001;22:519–23.
[23] Tong X, Zhao H, Tang T, Feng Z, Huang B. J Polym Sci, Part A: Polym Chem 2002;40:1706–11.
[24] Lim SK, Kim JW, Chin I, Kwon YK, Choi HJ. Chem Mater 2002;14: 1989–94.
[25] Kim JW, Kim SG, Choi HJ, Jhon MS. Macromol Rapid Commun 1999;20:450–2.
[26] Kim JW, Kim SG, Choi HJ, Suh MS, Shin MJ, Jhon MS. Int J Mod Phys B 2001;15:657–64.
[27] Kim TH, Jang LW, Lee DC, Choi HJ, Jhon MS. Macromol Rapid Commun 2002;23:191–5.
[28] Kim JW, Noh MH, Choi HJ, Lee DC, Jhon MS. Polymer 2000;41: 1229–31.
[29] Park JH, Lim YT, Park OO. Macromol Rapid Commun 2001;22: 616–9.
[30] Yeh JM, Liou SJ, Lai CY, Wu PC, Tsai TY. Chem Mater 2001;13: 1131–6.
[31] Kim BH, Jung JH, Joo J, Epstein AJ, Mizoguchi K, Kim JW, Choi HJ. Macromolecules 2002;35:1419–23.
[32] Sun Y, Ruckenstein E. Synth Met 1995;72:261–7.
[33] Sohn JI, Kim JW, Kim BH, Joo J, Choi HJ. Mol Cryst Liq Cryst 2002; 377:333–6.
[34] Kim JW, Liu F, Choi HJ. J Ind Engng Chem 2002;8:399–403.
[35] Kohlman RS, Joo J, Min YG, MacDiarmid AG, Epstein AJ. Phys Rev Lett 1996;77:2766–9.
[36] Joo J, Lee JK, Lee SY, Jang KS, Oh EJ, Epstein AJ. Macromolecules 2000;33:5131–6.
[37] See H, Kawai A, Ikazaki F. Colloid Polym Sci 2002;280:24–9.
[38] To K, Choi HJ. Phys Rev Lett 1998;80:536–9.
[39] Choi HJ, Cho MS, Kim JW, Kim CA, Jhon MS. Appl Phys Lett. 2001; 78:3806–8.
[40] Sim IS, Kim JW, Choi HJ, Kim CA, Jhon MS. Chem Mater 2001;13: 1243–7.
[41] Sohn JI, Sung JH, Choi HJ, Jhon MS. J Appl Polym Sci 2002;84: 2397–403.